Ignition and Detonation in Energetic Materials: An introduction.

William G Proud

Institute of Shock Physics, Imperial College London,
Prince Consort Road, London, SW7 2AZ, United Kingdom.

w.proud@imperial.ac.uk

Abstract: Theories on ignition and growth of reaction in energetic materials have developed significantly over the past two decades with increased experimental knowledge. There is an extensive and growing literature in this field. This paper deals with the fundamentals of the ignition and detonation process, highlighting the fundamental physics and chemistry of the situation. It is important to recognise that the overall processes may appear to be complex because they represent an interplay between thermodynamics and kinetics, the result is a dependance on pressure, temperature and time. In specific scenarios, high-shock wave levels for instance, one process may dominate but in general it is a combination of all three. The later section of this article discuss research relevant to this subject in greater detail.

1.1 Energetic Materials:

The term 'energetic materials' (EMs) often seems to be a euphemism for 'explosives' but actually describes a wide variety of materials. EMs can be divided into three broad categories; explosives, propellants and pyrotechnics. Explosives are defined as materials which react to produce a violent expansion of hot gas, an explosion, which rapidly delivers energy to its surroundings. The rate of transformation from solid to hot gas takes place on timescales of microseconds. Propellants are less violent in reaction and, as the name implies, are used to accelerate objects such as missiles and bullets; the time taken to go from solid to gas is of the order of milliseconds. Historically, some materials such as gunpowder can be used either as an explosive charge or as a propellant. The difference in behaviour being dependent on the amount of containment/confinement around the gunpowder; the more confined the more violent the reaction. Pyrotechnics are systems which react to produce an effect such as smoke, light or noise with reaction times from milliseconds to many minutes.

Comparing EMs with other materials such as petrol, 1 kg of petrol contains six times more available energy as the same mass of trinitrotoluene (TNT) *but* the TNT releases its energy a hundred million times faster. It is this rapid kinetics of transformation that forms the basis of explosion.

The simplest way to envisage the chemistry of an explosive is as a mix of an oxidiser with a fuel. Historically the most important explosive was gunpowder, classically having the ingredients potassium nitrate (the oxidiser), charcoal (the fuel) and sulphur (an initiatory compound making it easier for the mix to catch fire and stay lit). Burning between the grains of the different components, called deflagration, controls the rate of gas output.

In contrast, modern military and commercial explosives are based around materials which have the fuel and the oxidiser as separate chemical groupings on the same molecule, effecting a degree of mixing which is impossible to achieve with simple powders. This intimacy means that the reaction instead of moving as a flame, from grain surface to grain surface, now moves as a wave from molecule to molecule inside the explosive. The chemical reactions take place in a zone which is much less than 1 mm thick, fast moving at velocities of the order of 8000 m s^{-1} and at high-pressure of about 250,000 atmospheres (atm). This zone is called a detonation wave. The energy release rate is up to 1000 times higher than that for gunpowder. This high output rate results in these materials being called 'high order explosives' while gun powder which is deflagration-controlled, is a 'low order explosive'.

The output of an explosive can be defined in terms of two factors; brisance and heave. A shock wave can be transmitted from detonating high explosive into materials that cause them to shatter. This shattering is called brisance. In general this only happens when the explosive and target material are in physical contact, e.g. the rock around an explosive-filled borehole in a quarry or the metal casing of a shell. The second effect is produced by the expansion of the hot, gaseous products which lift, separate and throw materials; this is called 'heave'. For example, 1 cm^3 of explosive can produce approximately 10 litres of hot gas, an expansion of 10,000 times. Most explosive devices produce both brisance and heave. Military explosives tend to have more brisance and less heave. In this case the aim is to first shatter the target directly or to fragment a shell casing, afterwards accelerating those fragments.

1.2 Hot-spot formation

In general it is thought that the impact mechanisms by which explosives ignite and ultimately detonate are thermal in origin. The mechanical energy is envisaged as being converted into heat in localised regions by rapid or large deformations with the formation of 'hot-spots'. Although there is a wide agreement that hot-spots are the process by which energetic materials ignite the precise mechanisms have been open to discussion [1,2]. The following mechanisms are widely accepted; adiabatic compression of trapped gas spaces, viscous heating of material extruded between impacting surfaces, friction between grains of material and localised adiabatic shear of material. To these mechanisms other non-mechanical processes such as electrical discharge or laser-heating can be added.

In all cases the difference between critical and sub-critical hot-spots needs to be drawn. In the case of a critical hot-spot the reaction site is of sufficient size that the heat loss via thermal conduction is lower than the energy produced by the chemical reactions. Thus the reaction zones become larger and extend into the bulk material. Sub-critical hot-spots are those for which, while chemical reaction may break out, the heat loss from the region is higher than the production rate from the reactions. Thus the reaction is quenched.

In liquids, the conditions for critical hot spot formation have been extensively studied [3-8] and the size, duration and temperature required have been reasonably well-quantified. One advantage of a liquid or a single crystal of explosive is the inherent homogeneity of the system and relative ease of visualisation of the reaction front. However, many explosive systems are heterogeneous and energy concentration relies on an interplay between the components.

Calculations [9] and experiments [10] on single cracks growing in individual energetic crystals show that the energy released from the crack tip is not sufficient on its own to cause sustained reaction. However, friction caused by the rubbing of the fracture surfaces against one another after crack growth is an important mechanism in the production of hot-spots.

1.3 Detonation.

A detonation is best defined as a reactive shock wave. A shock wave is a high intensity pressure pulse which moves super-sonically, with respect to the sound speed, in the uncompressed medium. The speed of sound in water is around 1,500 m s^{-1}, a shock wave would move faster than this e.g. 1,600 m s^{-1}. The 'reactive' element of the description refers to the sense that the energy from the detonation is sustaining the pressure in the detonation wave and moving it forward. There are many ways of representing the process of a detonation but a relatively straight-forward way is to consider the pressure-volume relationship for an explosive.

In the figure 1(a) there is one line and two curves. The line is the Rayleigh line and represents the locus on which mass and momentum are conserved for a detonation wave. The slope of the line is related to the detonation wave speed, the density of the explosive and the sound speed in the explosive. The lower curve is the unreacted Hugoniot and it represents the conservation of energy for the unreacted material under shock loading. It can be seen that there are two points where the line crosses the unreacted Hugoniot – these are the

only two places where mass, momentum and energy are conserved and so represent the shocked and unshocked states of the material. Any other place in this graph would imply that one of the conservation laws is being broken and so would be 'unphysical' (i.e. not possible for a single shock wave).

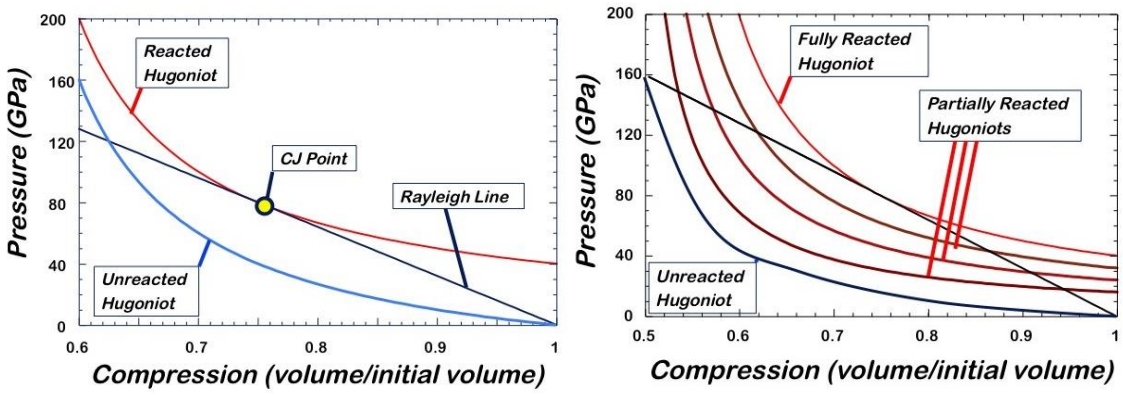

(a) (b)

Figure 1 (a) Pressure-volume graph of detonation explosive, instantaneous reaction (b) Pressure-volume graph of detonation with kinetics

When a high-explosive detonates, the molecular bonds are rearranged, producing a large energy release, giving a hot-high pressure gas: the detonation products. As the products are hot and, for a gas, very compressed, the curve representing the conservation of energy here, the reacted Hugoniot, occupies a region in the pressure-volume curve above that of the unreacted material. However, mass and momentum must be conserved so the Rayleigh line and the reacted Hugoniot must meet. This meeting point is called the Chapman-Jouget point (CJ point) and is the simplest case possible where mass, momentum and energy are conserved, this is the basis of C-J detonation theory.

It is possible to draw reacted Hugoniots that cross the Rayleigh line at two points. This is possible, does not violate any conservation laws and is seen in practical situations as over-driven detonation waves, corresponding to pressures above the CJ point and low velocity detonation which occurs at pressures below the CJ point. While possible, both these situations are, to some extent, unstable and often systems will revert to the detonation velocity associated with the CJ point.

A more realistic situation is where the detonation wave initiates a reaction which takes place over a finite amount of time. This was independently developed by Zeldovich, von Neumann and Deoring in the mid-1940's and is called ZND theory. This results in the pressure profile having a structure over the early stages, at the early stage the material is basically unreacted, however, it rapidly moves across a series of states to reach the fully reacted state, figure 1(b). This results in a pressure spike at the, called the von Neumann spike. Figure 2(a) shows such a spike measured in high-explosive by F. Bauer in 2001 [11]. This measurement required the use of in-material stress sensors and metal-coated explosives to eliminate electro-magnetic pick-up in the sensors from the detonation.

The above arguments apply to a one-dimensional system, all practical systems need to be considered as two- or three-dimensional. Explosives have a critical diameter; consider a cylinder of explosive below a certain diameter below the detonation will die out due to release waves coming from the long edge of the cylinder, effective 'energy leakage', reducing the stress and energy in the detonation wave, snuffing it out. For most military and commercial systems the aim of explosive engineers is to keep the explosive well above this critical limit.

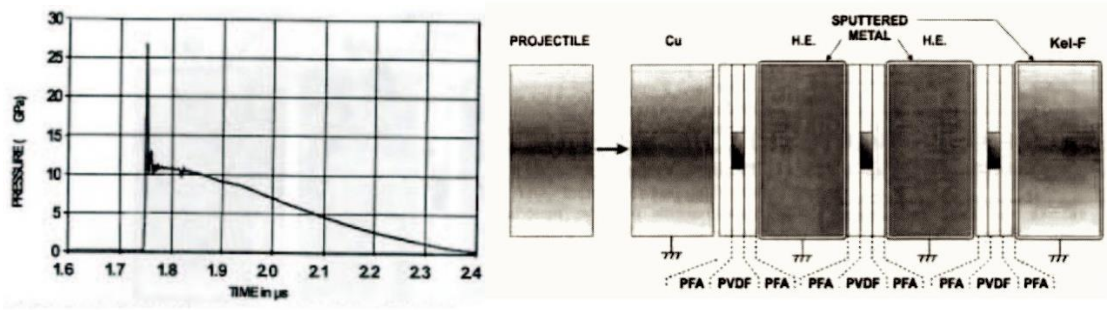

(a) (b)

Figure 2 (a) ZND spike seen in detonating high explosive (b) The experimental arrangement to obtain the ZND measurement. Taken from [11]

1.4 Deflagration to Detonation Transition.

Having recounted physical processes of hot-spot formation, leading to burning (deflagration) in the material and a brief review of detonation there is an obvious need for a linkage between the two. This linkage is extremely relevant to explosives research and engineering; determining, once the material has been struck, heated or subject to a shock wave, how do the hot-spots transition to a detonation wave. Some early research concentrated the build-up of burning, with increasing velocity, to full detonation. However, this faced the limitation shown in figure 3. The slope of the line of conservation of mass and momentum must have a negative slope in the pressure-volume space. However if the line is followed from the start condition ‘o’ to the reacted Hugoniot this needs a line with a positive slope. Such a gradient implies an imaginary density or velocity, i.e. a value multiplied by root of -1, and is non-physical.

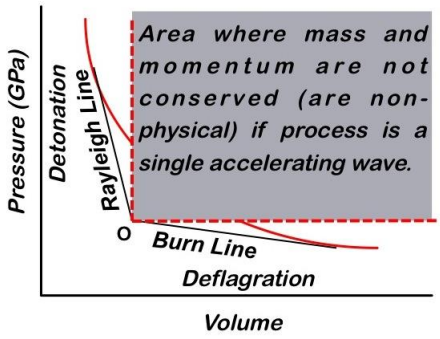

Figure 3 The problem of deflagration to detonation transition if the process is considered as a single wave.

However, this issue is based on the assumption that the reaction occurs as a single moving wave. It is necessary to consider the physical and chemical processes happening in the energetic material.

1.5 Process of Deflagration to Detonation Transition

One widely accepted mechanism for transition between deflagration and detonation (DDT) was described by McAfee *et al.* [12-15]. Here, the critical hot spots lead to deflagration, this is associated with conductive burning at a rate of order 0.01 m s^{-1} though the energetic material. There is also a faster convective burning, caused by product gases forcing open channels either pre-existing in powder compacts or produced by impact, it has also been seen that slow cook-off can allow such channels to develop over timescales of hours. This convective burning happens at velocities of order 10 m s^{-1}. The pressure associated with the convection wave also caused the material immediately in front of it to become compacted, represented by the compaction waves shown in figure 4(a), this slows the rate of gas percolation, but allows pressure, temperature and pressure to increase rapidly. This confined burning presses against the surrounding material forming a dense plug of material that is pushed into unreacted material. This plug forms a considerable number of compressed hot-spots in the unreacted material which cause a rapid pressure build up and a shock to detonation transition (SDT). SDT is discussed in more depth in the next section. A schematic of the process, from a column of granular material is shown in figure 4 with more detail to be found in [16] and in 2.1 (below).

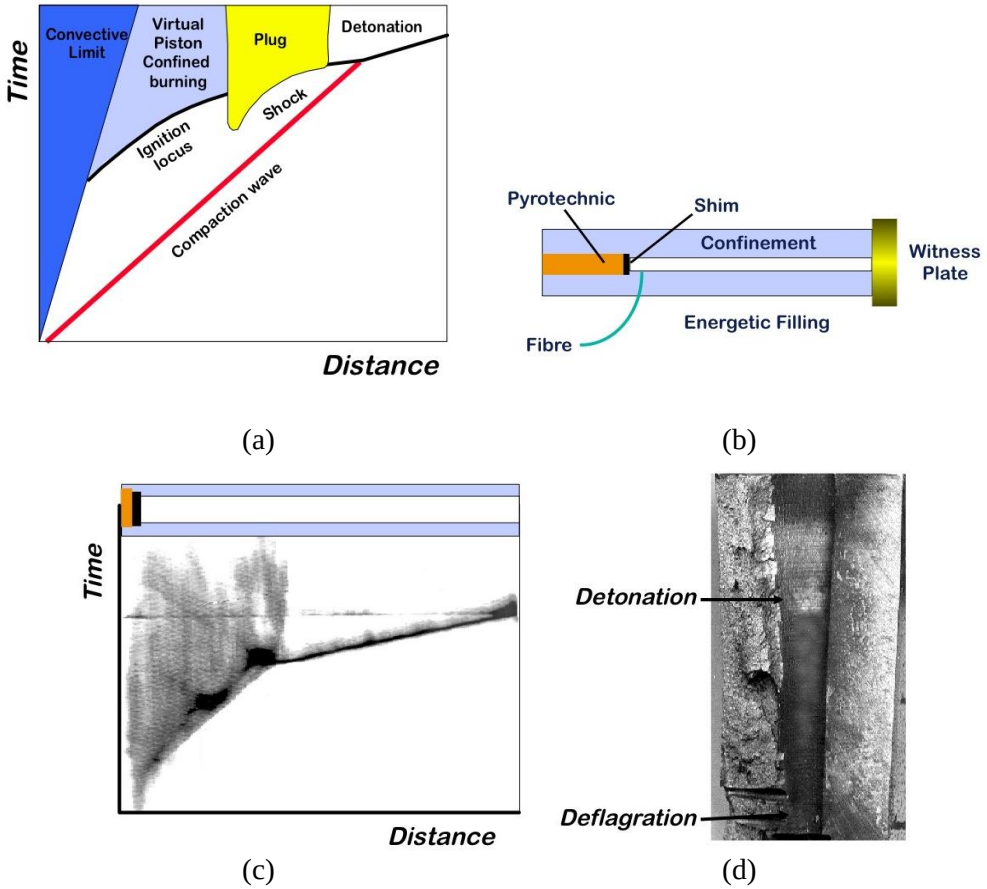

Figure 4. (a) Schematic of overall process proposed by McAfee et al.along the centre line of a sick of explosive. Distanece is the distance along the column from the ignition point, vertical axis is time, (b) Schematic of experimental arrangement used by Leubcke et al. [16], (c) Streak image showing deflagration to detonation transition, showing similarity with the schematic in (a), (d) recovered confinement showing smooth ring associated with the transition between deflagration and detonation.

The transit time between the deflagration and detonation depends on density of explosive, degree of confinement, nature of explosive, so is highly variable and subject to the precise local conditions. The

timescales for DDT is of milliseconds. A faster process which occurs for high-velocity impacts and stress is shock to detonation transition which occurs in microseconds.

1.6 Process of Shock to Detonation Transition

Shock to detonation transition (SDT) occurs in high-stress, shock wave environments. The process is effectively a thermal heating process. Shock waves are associated with rapid compression, high pressures and temperature rise. After a shock wave has passed over the material due to, for example, an impact, the region around the impact zone is subjected to a temperature rise which allows reaction to start via the shock heating. Again this can be considered as the formation of a considerable number of hot-spots which each send out pressure waves which can coalesce to produce a large pressure pulse. Effectively, thermal explosion occurs after an induction time depending on local conditions. When the detonation wave breaks out it runs through material already compressed and heated by the initial shock thus causing super-detonation, detonation at a higher velocity then that normally associated with the material. Eventually the reactive shock overtakes the original shock to produce overdriven detonation in the lower density material. Ultimately, this settles to the 'normal' detonation velocity over some relaxation time and distance.

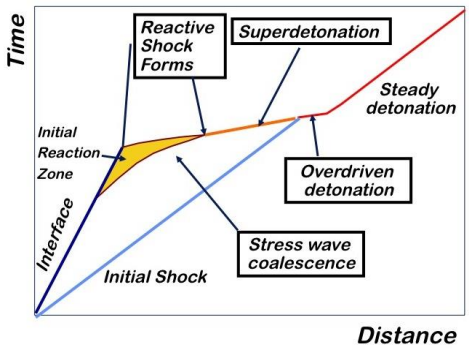

Figure 5. The process of Shock to Detonation Transition

2.1 Deflagration to Detonation Studies

Amongst the simplest experiments are those, which use metal cylinders as shown in figure 6. The channel along the centre of the cylinder had a diameter of 5 mm and varied in length between 70 and 100 mm (total length 100 - 130mm). Initial analysis of what had occurred while reaction had taken place in a column was performed by a system of post-mortem examinations. Test shots were carried out using cylinders made of copper, steel and brass. It was found that copper cylinders gave the best record of the event that had taken place. Brass proved too brittle to survive a detonation in one piece and steel although providing some record of the event did not distort in the ductile manner of copper and as such provided a less clear picture of the processes that had occurred.

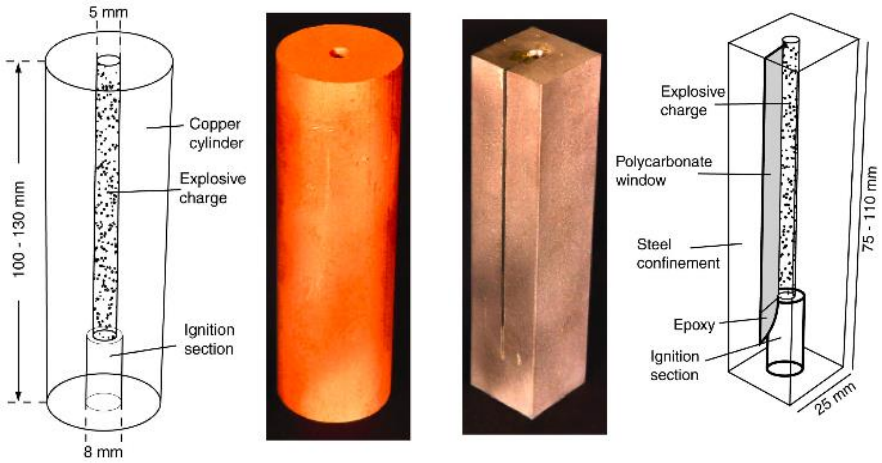

(a) (b)

Figure 6. Cylinders for use in (a) post-mortem type experiments (b) photographic study of DDT. Taken from [16]

Plastics such as polycarbonate and polymethylmethacrylate (PMMA) were not tried as it had been shown previously that the level of confinement offered by these materials was insufficient to withstand the sustained pressures required for a DDT event in PETN or RDX. In experiments where a photographic record of the events was required, it was necessary to use a confinement that afforded direct optical access to the charge whilst retaining the pressure levels of the simple metal confinement.

The confinement shown in figure 6(b) was developed by Luebcke [16] based on previous designs by researchers such as Korotkov [17] and Griffiths and Groocock [18]. The confinements used consisted of sections of square steel bar with a 5 mm channel drilled along the centre for the charge and a 1 mm wide polycarbonate window laid into the steel. The window affords an optical viewing point whilst being thin enough that the level of confinement afforded by the steel is not overly compromised. The length of the charges used varied from 45 to 80 mm depending on the nature of the event that was being investigated.

The explosive charges were pressed incrementally using a hydraulic press. Care was taken to ensure that the height of each individual increment never exceeded more than half of the diameter of the column. Charges below densities of 50% of theoretical maximum density (TMD) were also incrementally pressed. A system whereby static weights were placed on top of the pressing rod was used in these cases. A pyrotechnic was used to ignite the columns of explosive. The pyrotechnic was ignited using a nichrome wire through which was passed an electrical current. The mixture consisted of 80% potassium dichromate and 20% boron as developed by Dickson [19]. It has the advantage of producing few gaseous products, so little pre-pressurisation of the charge occurs. The burning temperature is far higher than the ignition temperature of the materials used in the charges. The pyrotechnic was tamped in order to ensure as few gas pockets as possible so as to reduce rapid expansion during reaction. The pyrotechnic was added after the main charge had been pressed into the column. Finally a small conical aluminium piece was placed around the electrical wires and pushed into the confinement to reduce rearward venting of the charge to a minimum. As a result pressure generated during the early stages of reaction could be sustained.

Often, a thin piece of copper foil was placed between the pyrotechnic charge and the explosive charge. This was done in order to prevent light emitted during the slow burning of the pyrotechnic charge from being transmitted down the column to the optical fibres and as a result prematurely triggering the experimental diagnostics. The brass tube into which the pyrotechnic charge was placed also acts as a light stop as well as an easy check on the amount of pyrotechnic that is used.

The type of data recorded from this experiment is shown in figure 7. A full description of the processes can be found in the papers of Gifford [20-22]. However, the streak image shows convective burning B, the step from deflagration to detonation D and the movement of the waves including a retonation wave F. Addition of high-speed thermocouples [21] to the system allowed the internal states at point along the column to be known prior to detonation.

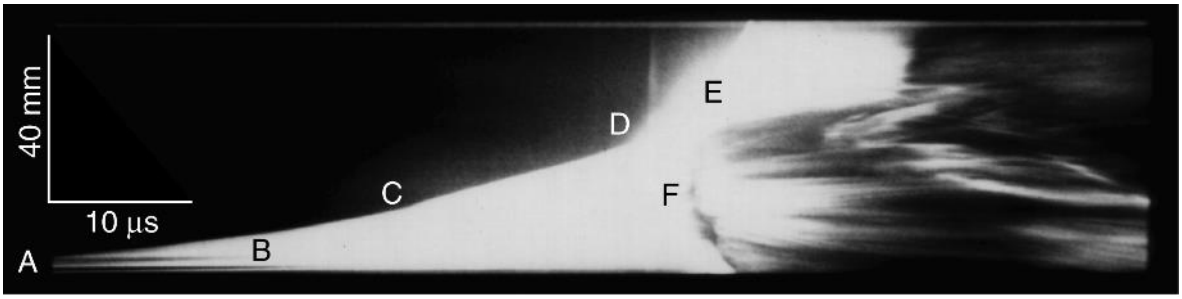

Figure 7. 'Normal' or type I DDT event in ultrafine PETN. Taken from [21]

2.2 Drop Weight Studies

A standard technique for sensitivity studies, the drop-weight is a system that allows long, low-level pressure pulses to be applied to small samples. In combination with high-speed photography, photodiodes and stress transducers it is a powerful system for both qualitative and quantitative analysis of material response.

The standard way of analyzing the output of a drop weight assumes the weight behaves as a rigid body and hence that one can simply apply Newton's laws of motion. This is used in determining the calibration of a drop weight force transducer dynamically, by directly relating the measured force both to the deceleration of the weight also to position.

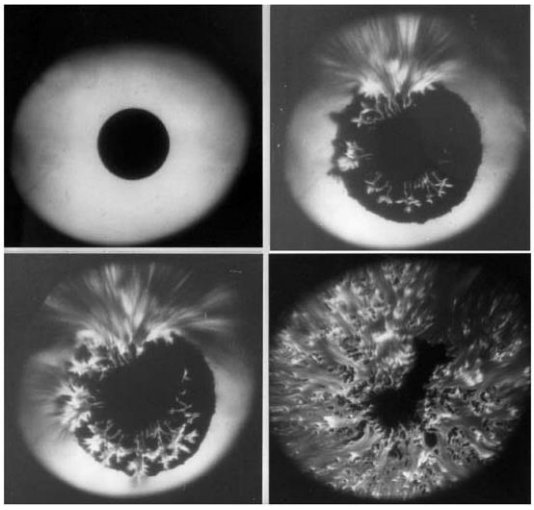

Figure 8 The ignition under impact of a thermite composition. Taken from [31]

In practice, the output signal from a drop weight machine often has oscillations comparable in size to the signal produced by the mechanical resistance of the specimen. This is particularly true if the drop weight itself is instrumented, e.g. with accelerometers. The reason is that impact excites the weight below its resonance frequency [23]. Elastic waves, therefore, reverberate around inside until the momenta of the

constituent parts of the weight have been reversed. Rebound then occurs and the specimen is unloaded. Recent work [24] has demonstrated that it is possible to obtain high quality data from such machines either by the use of a momentum trap in the weight, if the weight itself has to be instrumented [25] or by careful design of a separate force transducer placed below the specimen e.g. in [26,27].

One modification to the drop weight apparatus, which has proved invaluable in the elucidation of explosives ignition mechanisms, is to machine a light-path through the weight and to perform the deformation between transparent glass anvils [14, 28–31]. This allows the event to be captured using high-speed photography. An example of a 'classic' high-speed photographic sequences obtained using this apparatus is given in Figure 8.

2.2 Second Harmonic Generation

In a recent paper the use one of the more unusual optical properties of HMX to probe the ignition process [32]. The relatively new technique of Second Harmonic Generation (SHG) was used to study the β–δ phase transition in HMX by many authors in the late 1990s [33–36] A second harmonic is generated when intense radiation is incident on molecular crystals with appropriate symmetry properties. β-HMX, the "chair" configuration, is a centrosymmetric molecule and as such is forbidden by its symmetry from generating second harmonics. However, δ-HMX, a "boat" configuration, has no centre of inversion and generates second harmonics very efficiently. For these second-order processes to be observable the incident radiation needs to be very intense and so a laser is required. In order to produce second harmonics near the peak sensitivity of the high-speed cameras, a Nd:YAG, (YAG = yttrium aluminum garnet) laser operating at 1064 nm was used to irradiate the sample allowing the detection of the second harmonic at 532 nm (green). This technique can be applied in a transparent anvil drop weight apparatus. The second harmonic generation is near instantaneous process and so a 9 ns laser pulse, can a probe for δ-HMX during impact.

The apparatus allowed separate light paths for the laser light to travel to the sample and for the visible light (both light from reaction and SHG) to travel from the sample to the cameras. A diagram of the drop weight setup is shown in Figure 9.

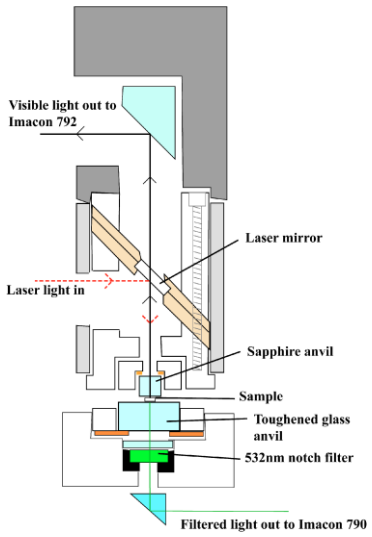

Figure 9. Drop weight modified to detect SHG in HMX crystals during impact. Taken from [32]

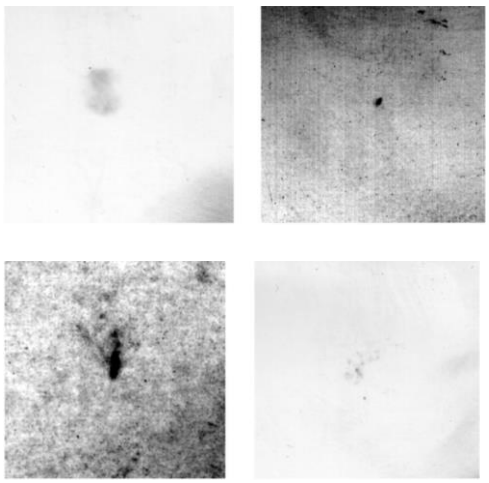

Figure 10. Four images showing SHG. The field of view of each image is 10 mm wide. All of the images have enhanced and reversed contrast (black indicates the presence of SHG). Taken from [32]

The cameras used were Imacons 790 and 792, and a notch filter in front of one of them was used to isolate SHG, while the other followed the visible light from reaction. A drop height of 39 cm was used, giving an impact velocity of 2.75 m s^{-1}. The height was chosen as the lowest at which the sample would reliably ignite on impact. The stress-time output was a half sinusoid with a peak pressure of 10^7 Pa and duration of the order of 10^{-4} s. A light gate broken by the falling drop weight just before impact was used to trigger the diagnostics, and a photodiode monitored the time of ignition relative to that time reference. While precise impact times are not known for individual experiments, the photodiode gave a good reference as to when reaction began. The system was such that one frame on the filtered camera coincided with the laser pulse. The visible light camera was set to record a sequence starting just before the laser pulse. Each pulse deposited 0.8 J of energy over an 8 mm diameter spot.

The sensitivity of the system to the presence of δ-HMX, in the sample bulk, was shown by using β-HMX pellets converted to δ-HMX through selective heating. SHG was clearly visible whether the δ phase regions were on the top or the bottom of the pellet and so δ -HMX at any depth in the sample could be detected with excellent spatial resolution in pellets up to 1 mm thick.

The time delay between the trigger provided by a light gate broken by the falling drop weight and the laser pulse was varied, in order to probe for δ-HMX throughout the impact. Selected images showing SHG are presented in Figure 10. The images showed the second harmonic in narrow regions of the sample. In the experiments all the impacted pellets reacted but no δ-HMX was observed any earlier than 13 μs before ignition. This implies that any transition to the δ phase occurs late in the reaction sequence. It could be the case that either the δ-HMX region grows rapidly before ignition or that after ignition the higher temperature of the burning material converts the rest of the sample before it is completely consumed.

In earlier research, Field [37] saw localized heating along lines and at their junctions and attributed this to shear band formation. It appears that the heating on impact is sufficient to cause conversion to δ phase under these stress conditions before ignition, the patches of δ-HMX observed were small (1 mm across) and very localized. After ignition, larger patches (3 mm across) of δ-HMX were seen before the sample was completely consumed.

2.4 Impact Ignition

In this study [38] ammonium nitrate was place in the impact cell shown in figure 11. This contains a bed of ammonium nitrate 0.2 mm thick. The front plate was a copper plate 2 mm thick and the rear glass window was 25 mm thick. A mirror, at 45˚ to the rear of the cell, directs light into a high-speed camera.

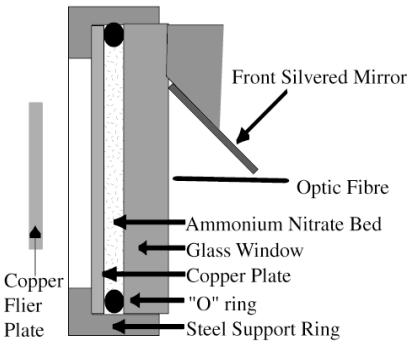

Figure 11 Impact cell used for ammonium nitrate studies.

The cell is mounted in at the end of a 19 mm bore gas gun. The flier plate was a 2mm thick copper plate mounted on a nylon sabot. The pressure in the impact chamber can be left at atmospheric pressure or pumped to a vacuum of 10^{-3} bar. The flier plate was aligned to the cell to a tolerance better than 0.05°. The width of the stress pulse imparted into by the impactor is of the order of 600 ns, this being sufficient to produce sustained reaction in the system. It was decided to reduce the bed thickness to 0.4 mm, corresponding to a bed thickness of 2-3 grains. This allowed the bed to be observed in its full depth. Tests revealed that the reaction build-up in the thin bed was the same as in previous experiments.

In figure 12 the result of an impact on a thin bed at 700 m s^{-1} is shown. The exposure time of each image was 30 ns and the interframe time was zero, as allowed by the Ultra-8 camera. Six frames are shown. Figure 13 shows the first two frames in detail, the first frame shows a number of regions of intense light output while in the second frame some of these regions in the top of the image have joined together. Other regions where the hot-spots are more widely spaced, towards the centre of the image, have died out. This appears to represent a distinction between critical and sub-critical hot-spots. Those hot-spots which are in proximity to one another link together possibly as a result of pressure pulses travelling between the hot-spots as a result of the production of product gases. Hot-spots which are more widely spaced tend to be quenched. In the third frame the reaction front has spread to cover about 55% of the impact area. In the later frames the reaction moves away from the central zone where the AN has been burnt.

This framing sequence provides strong evidence for the formation of both critical and sub-critical hot –spots. It is possible to use these images and count the hot-spot density and also measure the degree of interaction between individual hot-spots.

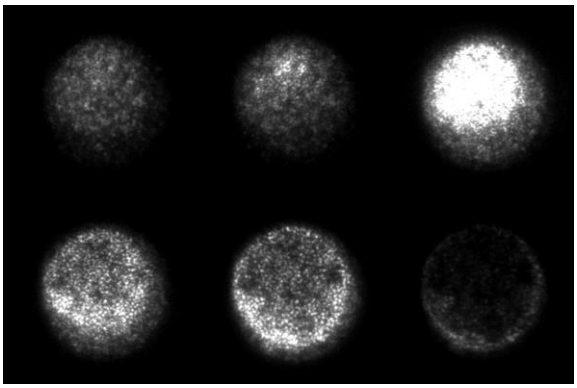

Figure 12 High-speed sequence of reaction in a 0.4 mm bed of AN grains, 150 – 210 μm in size, struck by a copper impactor at 700 m s^{-1}. Exposure time of each frame 30 ns. Frames are in order left to right, top to bottom. Diameter of reaction zone viewed approximately 8 mm.

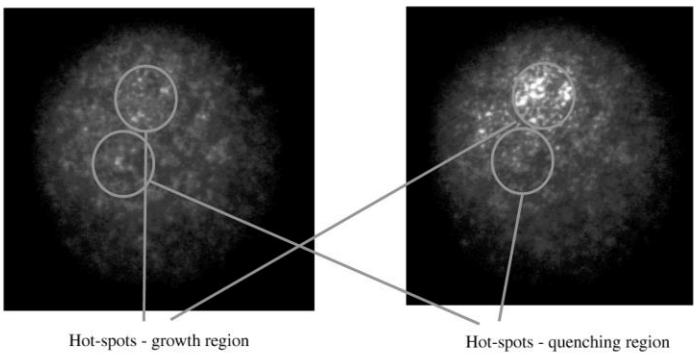

Figure 13 Detail of the first two frames of the sequence in figure 12. Areas where hot-spots are growing and those where hot spots are quenching are highlighted.

2.5 Small Scale Gap Test

In the last two examples, shock waves will be considered; a detonation is by definition a reactive shock wave. These examples are complementary. In the small-scale gap test a shock impinges onto a column of energetic material, while in the cylinder test an energetic material pushes on an inert surround cylinder of inert material.

The gap test is a shock sensitivity technique in which a sample of the material of interest is placed in contact with a barrier. On the other side of the barrier an explosive charge is detonated. The shock from the charge moves trough the barrier, losing energy as it goes, and, ultimately passes into the test material. The thicker the barrier, the more the pulse from the charge is reduced and the lower the shock felt by the sample. Experiments are repeated with different barrier or gap thicknesses until a 50:50, or other probability, go: no-go threshold is established.

In this study small samples were used [39]. The test samples were pressed into PMMA holders. The cylindrical holders were 25 mm long, 25 mm in diameter with a central bore of 5 mm. The columns were incrementally pressed with a step height of 0.5 mm to give a very homogeneous column. A variety of pressing densities were studied from 60% - 90%. The holders were then placed in the arrangement as shown in figure 14. The holder has a PMMA gap placed above it and a C8 detonator placed on top. The assembly was placed in an armoured box fitted with an observation window. The camera was triggered by a fibre optic that was fitted near the end of the detonator on top of the gap plate. When light was detected from this source, the camera was triggered. At the lower end of the gap arrangement, was a brass witness plate. All contacting surfaces were coated in a thin layer of silicone grease in order to allow good acoustic transmission between the layers.

The streak records from a series of experiments on 90% TMD PETN presented in figure 15. The PETN had an ultrafine grain size. The gaps were 3.51, 3.63, 3.67 and 3.71 mm. It can be seen that in the top image the detonation is slightly overdriven and was prompt i.e. at the top of the column. The detonation speed then settled down within 5 mm in the column length. In the second image, there is a slight hooking at the top of the column. This is due to the detonation not starting at the top of the column but rather a short distance down it. At 3.67 mm the hooking is severe and the detonation wave breaks out about 8 mm down the column. Finally at 3.71 mm there is no light associated with the detonation process. The brass witness plate dented in the area exposed to the explosive column indicating a detonation pressure in all cases except 3.71 mm. For 3.71 mm, only a small dent was seen indicating the more modest pressure associated with deflagration.

A similar series of results was obtained for conventional grain size material where the gap thickness for failure was shown to be 5.54 mm of PMMA. In a final series of experiments, Dynasen PVDF gauges [40] were placed between a gap plate and a block of PMMA 100 mm square and 25 mm thick, figure 16. The output from a PVDF gauge is shown in figure 20. The output voltage can be converted to stress. For the 5.54 mm gap used in the experiment here this corresponded to a stress level of 2.1 GPa. For a PMMA thickness of 3.67 mm, the stress level was of the order 4.1 GPa. It should be pointed out that the PVDF gauge is recording the stress for several microseconds, much longer than it takes detonation to start.

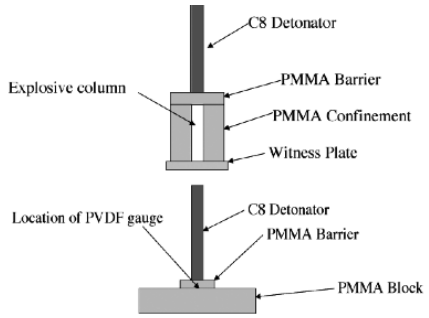

Figure 14. Experimental arrangements. Top, for gap test, Bottom, for PVDF gauge study

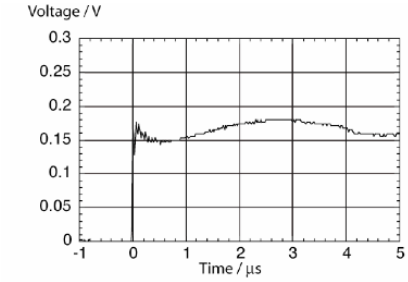

Figure 16. PVDF Output from a gauge separated by 5.54 mm PMMA gap from a C8 detonator.

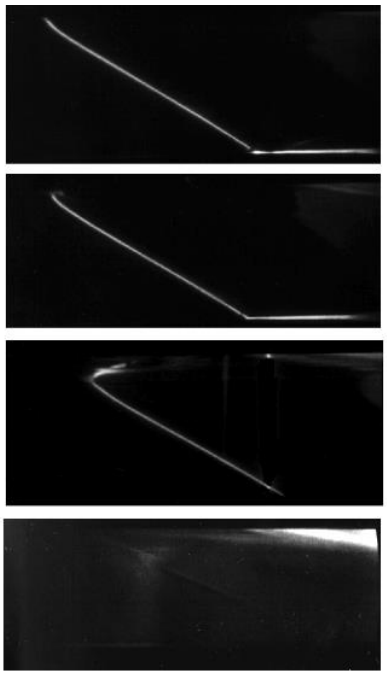

Figure 15. Streak records of fine-grained PETN 90% TMD. Variation in gap thickness; top - 3.53 mm, second – 3.63 mm, third – 3.67 mm, bottom – 3.71 mm

2.6 The Cylinder Test

The cylinder test is used to measure detonation performance. In concept it has a very simple geometry: a tube filled with explosive. The material is detonated and, if possible, the deformation of the tube is measured and then related to the detonation pressure and velocity. High-speed recording systems, such as streak photography, allow the rate of expansion of the cylinder to be measured relatively straightforwardly.

However, if the aim is to track gradual changes in detonation behaviour of a system, due to the presence of additives, especially in the width of the detonation front, this requires a more time-resolved technique. In this case streak photography was supplemented by the used of velocity interferometer (VISAR) [41]. In this study it was used to look at the effect of aluminium added to sensitized nitromethane [42].

In these experiments the streak camera recorded the radial expansion of the cylinder while the particle velocity-time history of the outer surface of the cylinder during detonation was determined using VISAR, figure 16. The initial acceleration can be seen to take the form of a series of steps. These are due to the reflection of waves within the copper cylinder. This can be explained with reference to figure 17.

The detonation of the NM/Al mix causes the cylinder to expand. A shock wave is sent from the inner wall to the outer wall of the cylinder. This reflects at the outer wall as a release, which moves back towards the centre of the tube. When it reaches the centre it is reflected as compression due to the sustained pressure of the detonation products. Overall, the outer wall of the cylinder accelerates as a series of steps. The cylinder walls become thinner, ultimately shredding into fragments. This effect tends to obscure the step-like

structure at later times. Hence the system with the most rapid expansion shows the least resolution of the steps while the highest loading of Al caused the most easily resolved steps.

It is important that the surface is not polished to an optical finish because such a finish is unlikely to be preserved at the high stress and strains associated with the cylinder test. Barker et al. developed this technique in the late 60's and early 70's [43]. The reflected laser light is captured and split into two beams, one of which is passed through a glass cylinder known as an "etalon". Because the refractive index of glass is larger than that of air, the light in this beam is slowed down and hence delayed with respect to the other beam, which passes through air. If the target is stationary, the interference pattern will not change with time when the two beams are recombined. For an accelerating target, however, the reflected beam will be Doppler shifted. The time resolution of the VISAR data is 2 ns and the noise on the photo-multiplier produces an error of ±5 %.

Copper cylinder expansion tests were carried out on nitromethane / aluminium (NM/Al) compositions containing 20, 30, 40, 50 and 60% by weight aluminium. The NM used was Analar grade and the aluminium particles were spherical, with a mean size of 10.5μm. The mixtures were prepared by adding 5% by weight of polyethylene oxide to the NM to thicken it, thus helping suspend the aluminium, then adding the appropriate percentage of aluminium. The copper cylinders (304mm long, 25.4mm ID with a wall thickness of 2.6mm) were mounted vertically, sealed at the bottom end and initiated by a small booster pellet at the top.

The overall expansion was viewed with a Cordin-132 streak camera writing at 5.999 mm/μs. An argon flash bomb and diffusing screen were used to provide backlighting. There was a decrease in expansion speed as the particle loading density was increased with a marked change between 40% and 50% as shown in figure 18.

The accuracy of measurement of the initial expansion phase is limited by the resolution of the film. Analysis of the VISAR traces gave the velocity histories shown in figure 19. The traces are offset for clarity. The velocity history in these traces tends to flatten after 10 μs but this is due to the loss in sensitivity when the fibre is close to the expanding copper surface. The initial acceleration can be seen to take the form of a series of steps. These are due to the reflection of waves within the copper cylinder. This can be explained with reference to figure 17.

The detonation of the NM/Al mix causes the cylinder to expand. A shock wave is sent from the inner wall to the outer wall of the cylinder. This reflects at the outer wall as a release, which moves back towards the centre of the tube. When it reaches the centre it is reflected as compression due to the sustained pressure of the detonation products. Overall, the outer wall of the cylinder accelerates as a series of steps. The cylinder walls become thinner, ultimately shredding into fragments. This effect tends to obscure the step-like structure at later times. Hence the system with the most rapid expansion shows the least resolution of the steps while the highest loading of Al caused the most easily resolved steps.

While the VISAR data measure the rapid acceleration of the outer surface of the copper cylinder in the first few microseconds, the steps are not seen in the resulting streak displacement history. Part of the reason for this is that the stepped region corresponds to the first 2 μs of the process, where the displacements are very small.

From this simple analysis it can be seen that while the streak camera system is excellent for large displacements it would be difficult to capture the detail of the early acceleration using such a system. The displacements measured using the streak and VISAR can be combined as shown in figure 20.

Figure 16. The experimental set-up

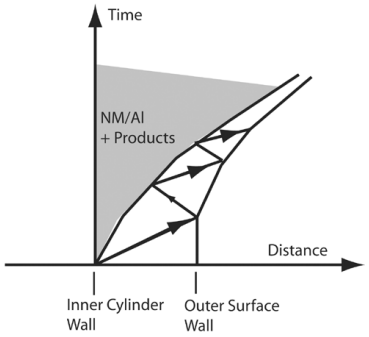

Figure 17 Schematic of deformation of the copper cylinder.

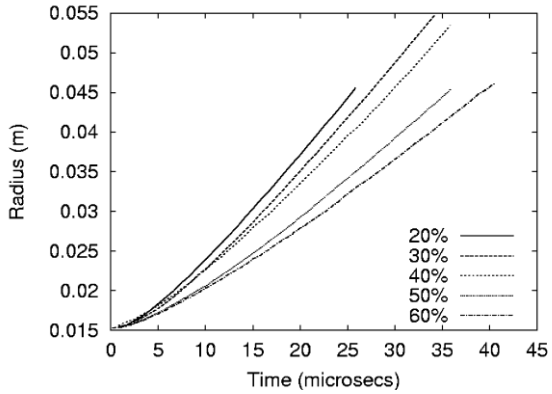

Figure 18. Streak camera records. Cylinder expansion radius time plots for various percentages mass fractions of 10.5 μm Al in nitromethane.

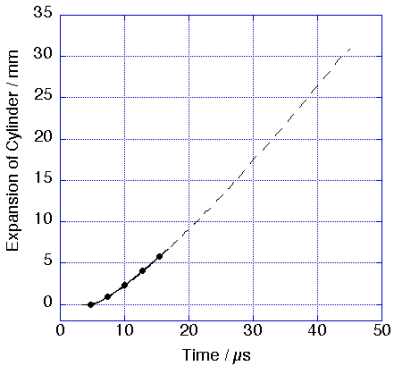

Figure 20. Combined VISAR (solid) and streak (dashed) records for 60% Al loading

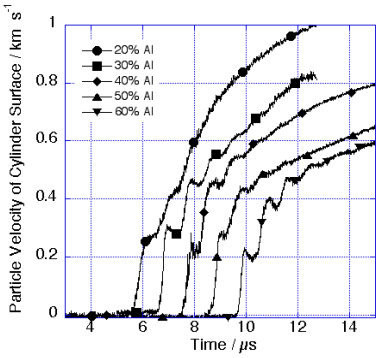

Figure 19. Velocity histories from VISAR for the loading densities studied

3.0 CONCLUSIONS

It is hoped that this article has introduced the field of deflagration and detonation studies. The first part concentrated on the fundamentals of this field while the second on active research areas.

While the above series of examples shows a wide range of techniques applied to energetic systems, ranging from low to high velocity impact, it is for from exhaustive. However, it is possible to draw some simple conclusions. Keeping experimental geometries and interfaces as simple as possible is useful as it allows data to be extracted with limited recourse to complex analysis. In energetic materials, it has been known for over 50 years that ignition and initiation are multi-variable processes and so experimental design is of paramount importance. In some cases like HMX, the specific crystal properties allow second harmonic generation to be used to look at the ignition process.

While many of the techniques listed can involve complex equipment, some advances, like the use of line lasers to monitor material expansion can be done with modest resources.

Finally, the desired output from the study is important, here the emphasis has been on experimental arrangement to understand fundamental processes so allowing a deeper understanding of how factors like composition affect the ignition and growth of reaction.

4.0 ACKNOWLEDGEMENTS

The author acknowledges the large number of colleagues, students and collaborators, who have supported and developed the techniques in this review, mainly at the Cavendish Laboratory, University of Cambridge. Principal inspiration and guidance was provided by Prof. J.E. Field. Other colleagues included Drs. And Profs. S.M. Walley, P.M. Dickson, N.K. Bourne, P.J. Rae, J.E. Blazer, S.G. Grantham, C.R. Siviour, H.T. Goldrein, D.J. Chapman, M.J. Gifford, P.E. Luebcke, H. Czerski, D.M. Williamson, E.J.W. Crossland all of whom contributed significantly. The late Dr. Avik Chakravarty made a singularly effective contribution to the small-scale gap test. Indispensable technical assistance was provided by D. Johnson, R. Marrah, R. Flaxman, K. Fagan and others. EPSRC, QinetiQ, [dstl], Orica, AWE and MoD, provided the support for much of this research. Drs and Profs. I.G. Cullis, A.S. Cumming, P. Gould, P.D. Church, D. Mullenger, P. Haskins, M. Cook, M. Braithwaite, all provided programmatic guidance. This list is not exhaustive and the author apologises for any omissions. The Institute of Shock Physics acknowledge the support of the Atomic Weapons Establishment, Aldermaston, UK and Imperial College London. Readers are asked to consult the original papers to find greater detail and attribution.

5.0 REFERENCES

[1] F. P. Bowden and A. D. Yoffe, Initiation and Growth of Explosion in Liquids and Solids (republ. 1985) (Cambridge University Press, 1952).

[2] J.E. Field, G.M. Swallowe and S.N. Heavens, Ignition mechanisms of explosives during mechanical deformation, Proc. R. Soc. Lond. A 382 (1982), 231-244

[3] F. P. Bowden and M. P. McOnie, Formation of cavities and microjets in liquids and their role in initiation and growth of explosion, Proc. R. Soc. Lond. A **298,** 38-50, 1967.

[4] G. D. Coley and J. E. Field, The role of cavities in the initiation and growth of explosion in liquids, Proc. R. Soc. Lond. A **335,** 67-86, 1973.

[5] N. K. Bourne and J. E. Field, Bubble collapse and the initiation of explosion, Proc. R. Soc. Lond. A **435,** 423-435, 1991.

[6] E. Wlodarczyk, Analysis of the efficiency of initiation of detonation by 'hot spots' generated by shock compression of gas bubbles included in the explosive. I: Analysis of the experimental data, J. Tech. Phys. **33,** 35-61, 1992.

[7] E. Wlodarczyk, Analysis of the efficiency of initiation of a detonation by hot spots generated by shock compression of gas bubbles included in the explosive. II: Theoretical analysis, J. Tech. Phys. **33,** 133-166, 1992.

[8] N. K. Bourne and J. E. Field, Explosive ignition by the collapse of cavities, Proc. R. Soc. Lond. A **455,** 2411-2426, 1999.

[9] W. Holmes, R.S. Francis and M.D. Fayer, Crack propagation induced heating in crystalline energetic materials, J. Chem. Phys., 110 , 3576-3583, 1999

[10] M.M. Chaudhri, J.E. Field, S.N. Heavens and M. Coley, Studies of the initiation of explosives using high-speed photography, 10th International Conference on High-speed Photography, 1972

[11] Bauer, F. (2000). Advances in PVDF shock sensors: Applications to polar materials and high explosives. Shock Compression of Condensed Matter - 1999. M. D. Furnish, L. C. Chhabildas and R. S. Hixson. Melville, New York, American Institute of Physics: 1023-1028.

[12] McAfee, M., et al. (1989). Deflagration to detonation in granular HMX. Proc. Ninth Symposium (Int.) on Detonation. Arlington, Virginia, Office of the Chief of Naval Research: 265-279.

[13] McAfee, J. M., et al. (1991). Deflagration to detonation in granular HMX: Structure and kinetics in the predetonation region. Proc. 1991 JANNAF Propulsion Systems Hazards Subcommittee Meeting (CPIA Publ. 562). C. T. Hudson. Columbia, MD, Chemical Propulsion Information Agency: 153-162.

[14] McAfee, J. M., et al. (1995). Deflagration-to-detonation in granular HMX: Ignition, kinetics, and shock formation. Proc. 10th Int. Detonation Symposium. J. M. Short and D. G. Tasker. Arlington, Virginia, Office of Naval Research: 716-723.

[15] McAfee, J. M. (2010). The deflagration to detonation transition. Shock Wave Science and Technology Reference Library. 5: Non-Shock Initiation of Explosives. B. W. Asay. Berlin, Springer: 483-535.

[16] Luebcke, P. E., Dickson, P. M., et al. An experimental study of the deflagration to detonation transition in granular secondary explosives. Proc. R. Soc. Lond. A 448: 439-448 **1995**

[17] Korotkov, A. I., Sulimov, A. A., et al. Transition from combustion to detonation in porous explosives. Combust. Explos. Shock Waves 5: 216-222. **1969**

[18] Griffiths N and Groocock JM, The burning to detonation of solid explosives. J. Chem. Soc. 11: 4154-4162 **1960**

[19] Dickson PM, and Field JE, Initiation and propagation in primary explosives. Proc. R. Soc. Lond. A 441: 359-375. **1993**

[20] Gifford MJ, Proud WG, Field JE, Development of a method for quantification of hot-spots. Thermochimica Acta, Vol. 384 pp. 285-290. **2002**

[21] Gifford MJ, Proud WG and Field JE, Observations on type II deflagration-to-detonation transitions. Shock Compression of Condensed Matter - 2001. M. D. Furnish, N. N. Thadhani and Y. Horie eds. Melville, NY, American Institute of Physics: 878-881. **2002**

[22] Gifford, M. J., Luebcke, P. E., et al. A new mechanism for deflagration-to-detonation in porous granular explosives. J. Appl. Phys. 86: 1749-1753. **1999**

[23] Pope PH, Dynamic compression of metals and explosives. PhD thesis, University of Cambridge, **1985.**

[24] Follansbee PS, Regazzoni G, Kocks UF, The transition to drag controlled deformation in copper at high strain rates. Inst Phys Conf Ser;70:71–80. **1984**

[25] Heavens SN, Field JE. The ignition of a thin layer of explosive by impact. Proc R Soc Lond A;338:77–93. **1974**

[26] Field JE, Bourne NK, Palmer SJP, Walley SM. Hot-spot ignition mechanisms for explosives and propellants. Philos Trans R Soc Lond A;339:269–83. **1992**

[27] Walley SM, Field JE, Palmer SJP. Impact sensitivity of propellants. Proc R Soc Lond A;438:571–83. **1992**

[28] Walley SM, Balzer JE, Proud WG, Field JE. Response of thermites to dynamic high pressure and shear. Proc R Soc Lond A;456:1483–503. **2000**

[29] Czerski H, Greenaway MW, Proud WG, and Field JE, β-δ phase transition during drop weight impact on HMX. J. Appl. Phys. 96: 4131-4134. **2004**

[30] Henson, B. F., B. W. Asay, et al. Dynamic measurement of the HMX β-δ phase transition by second harmonic generation. Phys. Rev. Letts 82: 1213-1216. **1999**

[31] Saw CK, Kinetics of HMX and phase transitions: Effects of particle size at elevated temperature. Proc. Twelfth International Detonation Symposium. Arlington, VA, Office of Naval Research: 70-76. **2002**

[32] Smilowitz L, Henson BF, Asay BW, and Dickson PM, Kinetics of the β–δ phase transition in PBX 9501. Shock Compression of Condensed Matter - 2001. M. D. Furnish, N. N. Thadhani and Y. Horie eds. Melville, NY, American Institute of Physics: 1077-1080. **2002**

[33] Smilowitz L, BF Henson, et al. The β–δ phase transition in the energetic nitramine ocathydro-1,3,5,7-tetranitro-1,3,5,7-tetrazocine: Kinetics. J. Chem. Phys. 117: 3789-3798. **2002**

[34] Field J.E., Bourne, N.K., Palmer S. J. P., and Walley S. M. (unpublished).

[35] W.G. Proud, E.J.W. Crossland and J.E. Field, "High-speed photography and spectroscopy on determining the nature, number and evolution of hot-spots in energetic materials" Proc. SPIE 4948 (2003) 510-518

[36] Chakravarty A, Gifford MJ, Greenaway MW, Proud WG and Field JE, Factors affecting shock sensitivity of energetic materials. 12th APS Topical Meeting on Shock Compression of Condensed Matter 2001. M. D. Furnish, N. N. Thadhani and Y. Horie eds. Melville, NY, American Institute of Physics: 1007-1010. 2002

[37] Bauer, F. Advances in piezoelectric PVDF shock compression sensors: Applications to HE studies. Proc. 25th Int. Pyrotechnics Seminar. Saint Aubin, France, Association Française de Pyrotechnie: 28-37. **1999**

[38] Barker, LM and Hollenbach, RE, Laser interferometer for measuring high velocities of any reflecting surface." J. Appl. Phys. 43: 4669-4675. **1972**

[39] Proud, WG, Field, JE, Milne A, Longbottom AW, Haskins PJ, Briggs RI and Cook MD, The detonation of NM/Al mixtures. Proc. Fifth Int. Symp. on High Dynamic Pressures. Vol. 1. Paris, France, Commissariat à l'Energie Atomique: 135-141. **2003**